Earthquakes and Structures, *Vol. 13, No. 2 (2017) 165-176*
DOI: https://doi.org/10.12989/eas.2017.13.2.165

The multi-axial testing system for earthquake engineering researches

Te-Hung Lin[1a], Pei-Ching Chen[*2] and Ker-Chun Lin[1b]

[1]*National Center for Research on Earthquake Engineering, National Applied Research Laboratories, 200, Sec. 3, HsinHai Rd., Taipei 106, Taiwan*
[2]*Department of Civil and Construction Engineering, National Taiwan University of Science and Technology, No.43, Keelung Rd., Sec.4, Taipei 106, Taiwan*

(Received May 2, 2017, Revised July 2, 2017, Accepted July 3, 2017)

Abstract. Multi-Axial Testing System (MATS) is a 6-DOF loading system located at National Center for Research on Earthquake Engineering (NCREE) in Taiwan for advanced seismic testing of structural components or sub-assemblages. MATS was designed and constructed for a large variety of structural testing, especially for the specimens that require to be subjected to vertical and longitudinal loading simultaneously, such as reinforced concrete columns and lead rubber bearings. Functionally, MATS consists of a high strength self-reacting frame, a rigid platen, and a large number of servo-hydraulic actuators. The high strength self-reacting frame is composed of two post-tensioned A-shape reinforced concrete frames interconnected by a steel-and-concrete composite cross beam and a reinforced concrete reacting base. The specimen can be anchored between the top cross beam and the bottom rigid platen within a 5-meter high and 3.25-meter wide clear space. In addition to the longitudinal horizontal actuators that can be installed for various configurations, a total number of 13 servo-hydraulic actuators are connected to the rigid platen. Degree-of-freedom control of the rigid platen can be achieved by driving these actuators commanded by a digital controller. The specification and information of MATS in detail are described in this paper, providing the users with a technical point of view on the design, application, and limitation of MATS. Finally, future potential application employing advanced experimental technology is also presented in this paper.

Keywords: multi-axial testing system; degree-of-freedom control; advanced experimental technology; structural testing

1. Introduction

In recent years, the applications of energy dissipation and base isolation devices for buildings and infrastructures have been significantly increased in order to accommodate earthquake ground motions in high risk earthquake areas. These devices are expected to undergo large force and displacement responses during an earthquake. In particular, base isolation devices are subjected to large vertical force and lateral deformational simultaneously. The demand for conducting performance validation testing of these devices has been increasing; therefore, two well-known facilities were constructed to investigate dynamic characterizations of energy dissipation and base isolation devices. The first one is the seismic response modification devices (SRMD) located in the University of California at San Diego in US (Rich 1998), and the other one is the Bi-axial Bearing Tester System that was installed at the Università di Pavia in Italy. A large amount of performance tests of base isolation devices have been completed using the two facilities.

National center for research on earthquake engineering (NCREE) in Taiwan started to construct a multi-axial testing system (MATS) in 2007 as shown in Fig. 1. MATS is a 6-DOF testing facility, providing the capability of applying vertical, horizontal, and lateral loading as well as three directions of moment on a specimen. Therefore, MATS is capable of conducting a large variety of structural testing with realistic loading conditions. The basic design requirements of MATS are (1) vertical force must be larger than 40 MN, (2) horizontal force must be larger than 4 MN, and (3) horizontal displacement must be larger than 1.2 m. In this paper, the design and analysis of MATS are

Fig. 1 Aerial view of MATS under construction

∗Corresponding author, Assistant Professor
E-mail: peichingchen@mail.ntust.edu.tw
[a]Assistant Researcher
E-mail: thlin@ncree.narl.org.tw
[b]Researcher Fellow
E-mail: kclin@ncree.narl.org.tw

ISSN: 2092-7614 (Print), 2092-7622 (Online)

described in detail first, including the platen, post-tensioned columns, and reaction frame. Then, the capacity, and limitation of MATS are introduced. Afterwards, a large variety of experimental applications are presented, providing the users with the general aspects of experiments that have been conducted using MATS. Finally, future potential application that utilizes advanced experimental technology is also stated in this paper.

2. System components and analysis

As shown in Fig. 2, MATS is composed of a steel-and-concrete composite platen, a high strength self-reacting frame, and various kinds of servo-hydraulic actuators. It took a long time to make final decision of the self-reacting frame type in the design process. Finally, a high strength self-reacting frame consists of a steel cross-beam in-filled with high-strength concrete at the top, a reinforced concrete mat foundation at the bottom, and two A-shape post-tensioned reinforced concrete frames in the middle were designed. Excluding the steel cross-beam, the entire loading frame was made of reinforced concrete (RC) for the cost effectiveness. The reaction wall provides the horizontal reaction supports for horizontal forces applying to the platen of the MATS. For testing a full-scale RC column or steel column specimen, a 5.0 meter high and 3.25 meter wide clear space in MATS is provided. The specimens can be anchored between the cross-beam and the platen with a maximum allowable specimen height of 5 meters. Two large openings are made on both A-shape reaction frames as view windows in order to monitor of the specimen conveniently during the test.

MATS was originally designed for conducting testing of large-scale base isolators such as lead rubber bearings (LRB). However, three additional types of experiments were then considered using MATS in the final design scheme including high axial force demand with low or moderate shear deformation; low or zero axial force demand with moderate shear force deformation; and high axial force and velocity demands. Table 1 shows the four test types considered in the design of MATS. Case I, II, III, IV are base isolator test, RC column test, velocity-dependent damper test, and bracing member test, respectively. Fig. 3 show the free body diagram of a bi-axially loaded member during the test. Some assumptions and limitations of specimen's strength and displacement capacities were made. The notations of P, H, h_c and Δ represents the vertical load, the horizontal load, the distance from the top face of the platen to the midpoint of the specimen, and the maximum horizontal displacement, respectively. As shown in Table 1, two extreme categories of experiments were considered in the design of MATS. One is the bi-axially loaded test that requires high vertical force capacity (40 MN), moderate horizontal force (4 MN), and large horizontal displacement (±1.2 m). The other one is the uni-axially loaded test that demands low or zero vertical force, large horizontal force (8 MN), and moderate horizontal displacement (±0.5 m). After balancing the moment at the point O resulted from all forces, i.e., $\Sigma M_o=0$, the following equation can be obtained:

$$P_1 - P_2 = \frac{M_{P\Delta} - M_H}{1.8} = \frac{\frac{P\Delta}{2} - H\left(\frac{h_p}{2} + h_c\right)}{1.8} \tag{1}$$

After applying static analysis, 16 MN vertical load capacity for each side was necessary. However, the possibility of such an extreme situation was considered low. Consequently, three vertical actuators with 5 MN loading capacity were allocated in the final design. To satisfy the design requirements, the loading capacity of center actuator was 30 MN. Accordingly, there were a total of 7 vertical actuators, providing a total of 60 MN vertical force. In addition, four lateral actuators and two hold down actuator were configured to meet various testing purposes. Consequently, not only a multi-purpose testing facility has been built, but also a 6-degree-of-freedom controlled

Table 1 Four test types considered in MATS

Case	Test Types	P (MN)	H (MN)	Max. h_c (mm)	Min. h_c (mm)	Δ (mm)	Velocity
I	Base isolator (LRB)	40	4	750	250	±1200 ±500	Static Dynamic
II	RC column	40	4	2500	2000	±210	Static
III	Velocity-dependent damper	-	4	350	-	±500	Dynamic
IV	Brace element (BRB)	-	8	350	-	±300	Static

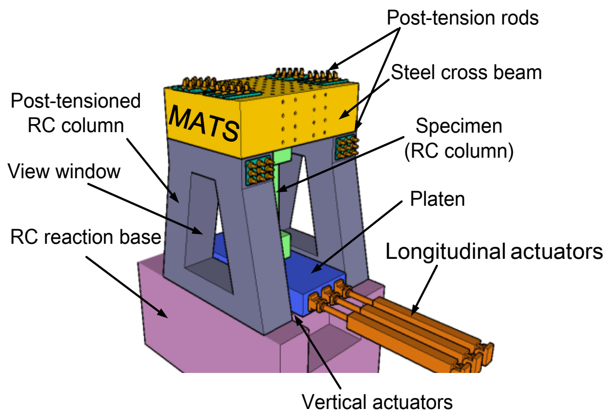

Fig. 2 Illustration of MATS components

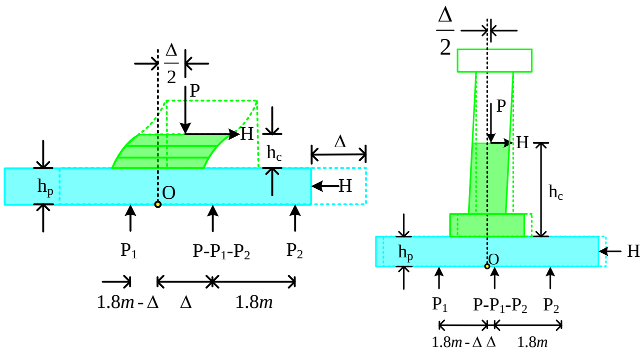

(a) Base isolator (b) RC column

Fig. 3 Free body diagram of bi-axially loaded member system has been developed. The analysis and design process of each part of MATS in detail are given below.

2.1 Platen

The platen is used to transfer actuators' forces and deformation to the specimen so that it can be subjected to compressive and shear forces as well as bending moments during testing. The platen design is critical because it highly affects the accuracy of a test. The dimension of the platen was designed as 6.7-meter long, 2.54-meter wide, and 0.9-meter high in order to match the pattern of mounting holes on the existing reaction wall. Fig. 4 shows the 3-D schematic of the platen interior. The platen consists of six exterior steel plates to form a box shape. The top flange and two side webs (in the longitudinal direction) are 50-mm thick. The two end plates (front and back sides) are 60-mm section beams were welded to the bottom, front, and back

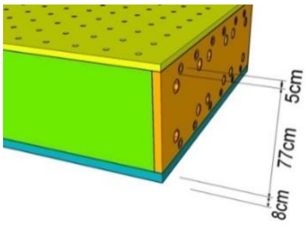

(a) Top and bottom flanges

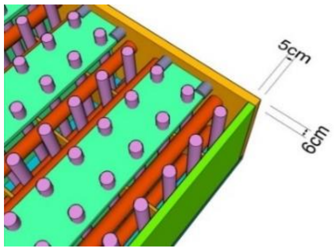

(b) End plates and side webs

Fig. 4 Three-dimensional simulation of the platen

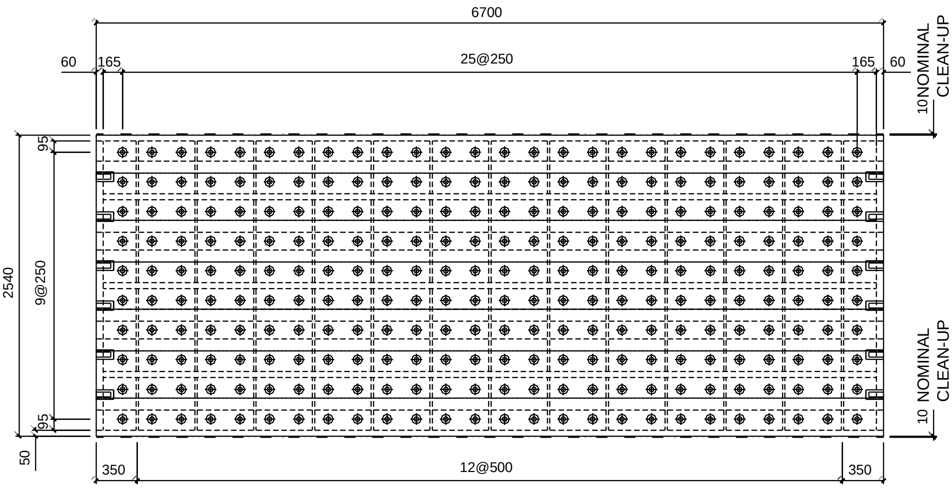

Fig. 5 Plan view of the platen

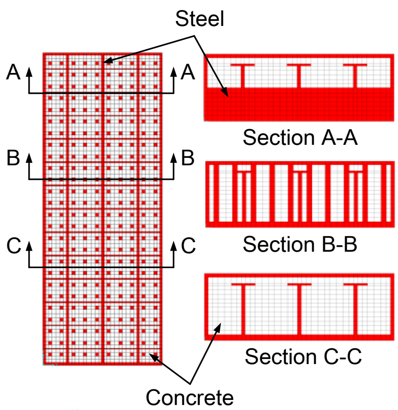

(a) Inside of the finite element model

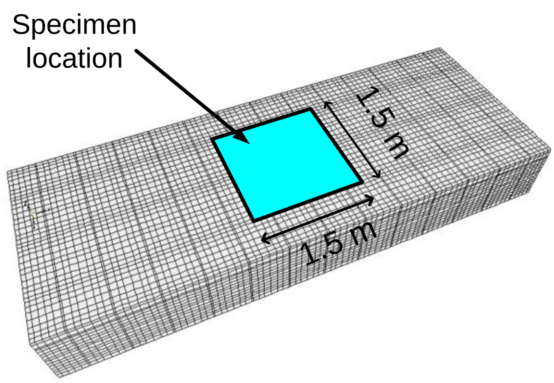

(b) Location of the specimen on the platen

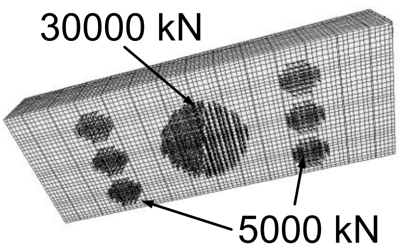

(c) Apply 60 MN vertical load under the platen

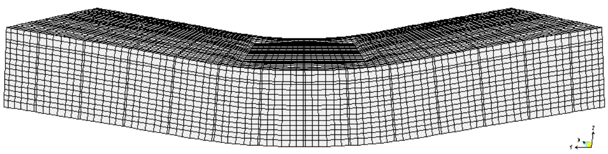

(d) Deformation of the platen under 60 MN vertical load

Fig. 6 Finite element model of the platen thick and the bottom flange plate is 80-mm thick. Three T-plates in the longitudinal direction. High strength concrete of 56 Mpa (8000 psi) was in-filled into the platen to enhance its stiffness and strength. In addition, 20-mm thick and 370-mm high stiffeners were welded to the bottom flange and two side webs with 500 mm spacing in the transverse direction. Steel rods with a diameter of 80 mm were placed with 250 mm spacing in two principal axes and welded at the top and bottom flanges. For mounting the specimen, threaded holes with 42-mm diameter and 100-mm depth were arranged at the top end of each rod as shown in Fig. 5. The deformation and the stress of the platen were investigated by performing finite element analysis using SAP2000. Maximum relative deformation of the platen at which the 5 MN and 30 MN vertical actuators were placed should not to exceed 0.0254 mm and 0.254 mm, respectively when the full hydraulic pressure was applied. Fig. 6 shows the finite element model of the platen. A 1.5 meter by 1.5 meter square specimen was assumed to locate at the center of the platen. Full vertical force capacity was applied at the location where the seven vertical actuators were placed. The analytical results indicated that the maximum overall deformation was 2.44 mm. Meanwhile, the maximum relative deformation of the platen at which the 5 MN and 30 MN vertical actuators were placed was 0.0267 mm and 0.1748 mm, respectively. Even though the analytical maximum relative deformation at the location where the 5 MN actuators were attached was slightly larger than the allowable maximum relative deformation; however, it was considered acceptable for the engineering application.

2.2 Post-tensioned columns

Four inclined reinforced concrete columns with a five to one slope ratio that were symmetrical to the center line of MATS were arranged to form the two side windows in the MATS frame. The dimension of each reinforced concrete column is 1.45 m x1.45 m. Based on the analytical results; a maximum pre-stressed force of 18.9 MN in the axial direction of each column was required. Twelve 75mm-diameter high strength post-tensioned rods were placed symmetrically in each column to provide at least 33.6 MN (2.8 MN per rod) pre-stressed force as shown in Fig. 7. It was critical to ensure that the column and the cross beam remain in contact even in the severest test condition. Therefore, the lower end of the post-tensioned rod was anchored within the concrete foundation while the upper end was anchored above the top flange of the cross beam. In addition, two pre-stressed concrete top cap beams with 1.45-m width and 1-m depth (as shown in Fig. 7) were constructed in the longitudinal direction to support the cross beam, transferring shear, moment and torque induced at the cross beam to the reaction columns. Each beam was post-tensioned by nine 40-mm diameter high strength post-tensioned rods, providing a total of 8.1 MN force to tie the two reinforced concrete columns.

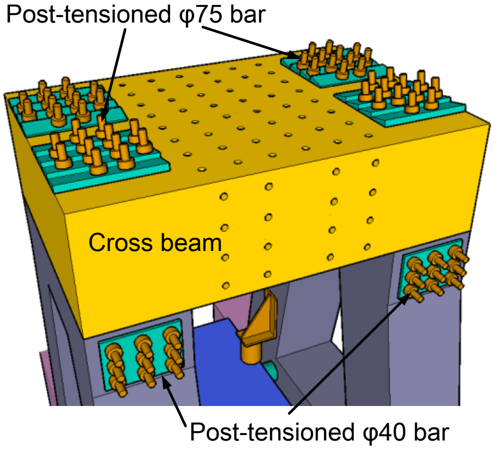

(a) Distribution of the rods

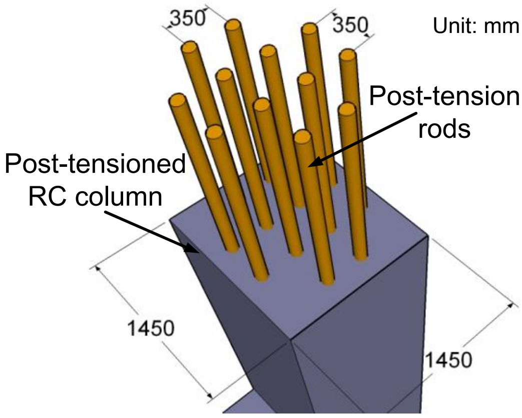

(b) Distribution of the rods in the RC column

Fig. 7 Crossbeam and the post-tension rods

2.3 A-frame and crossbeam

The cross beam located on the top of the MATS frame is used to mount the shim blocks or specimens, transferring the forces from the specimen to the two A-shape frames. The dimensions of the steel cross beam are 1.8 m in height, 6.15 m in width, and 4.3 m in length. The cross beam was constructed using steel plates with three different thicknesses: the flanges and two side webs were 50-mm thick; the stiffeners in the two sides were 25-mm thick; and the stiffeners at the center were 30-mm thick. Furthermore, 69 MPa (10,000 psi) high strength concrete was in-filled into the steel cross beam in order to increase the strength and stiffness of the cross beam, decrease the deformation of bottom plate, and prevent the stiffeners from buckling. The maximum considered torque at the center of the cross beam was 46.6 MN-m while a full-scale lead rubber bearing specimen was tested (case I in Table 1). Fig. 8 shows the plan view of cross beam. A total of 48 holes with an inner diameter of 93.6 mm were fabricated through the entire height of the cross beam in order to mount the RC or steel shim blocks or specimens under the cross beam for accommodating to the specimen height. The spacing of every two mounting holes is 500mm in the both horizontal directions. Besides, a total number of 16 holes with an inner diameter of 93.6 mm were fabricated on the two sides of the cross beam in order to connect to additional fixtures so that the clear space for mounting the specimen can be enlarged. The maximum allowable post-tension force of each hole was 2000 kN. The deformation and the stresses of the cross beam were also investigated by conducting finite element analyses using SAP2000. Fig. 9 shows the finite element model of the cross beam and the entire A-shape frame. Elastic shell and solid elements were used to simulate steel plate and concrete in the finite element model. The maximum vertical deformation and rotation of the cross beam should be less than 5 mm and 0.001 radian, respectively. The analytical results show that the maximum vertical deformation and rotation at center of the crossbeam was 2.2 mm and 0.00045 radian, respectively.

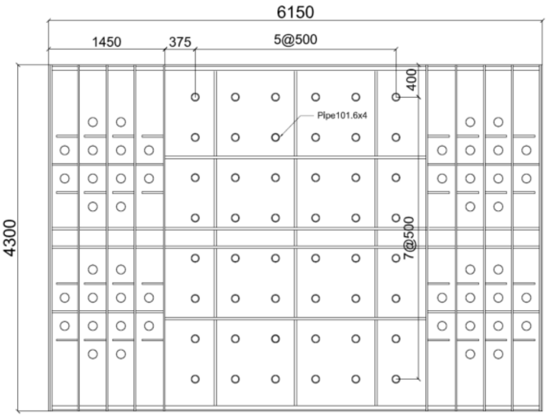

Fig. 8 Plan view of the crossbeam

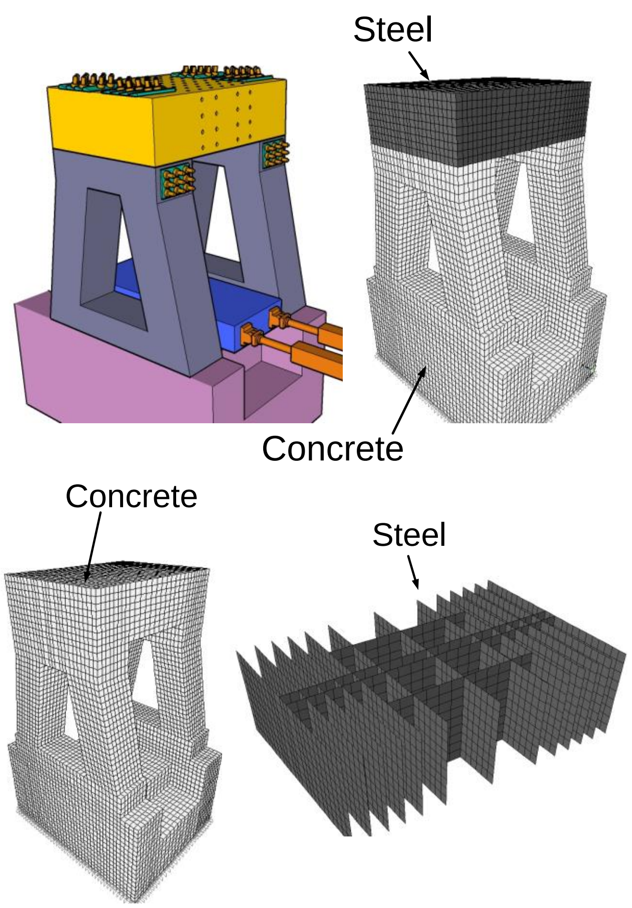

Fig. 9 Finite element model of the A-frame

3. Capacity and limitation of MATS

After several times of design iterations, MATS has been constructed as a 7.75-meter high and 6.15-meter wide testing facility. The maximum allowable specimen height is 5 meters. A post-tensioned and pre-stressed system is used to decrease the vertical deformation of the loading frame subjected to large vertical force. Fig. 10 illustrates the dimensions of MATS after the construction was completed. In this section, the capacity and limitation of MATS are introduced in detail, providing the users with a clear aspect for preparing specimens to be tested using MATS.

3.1 Force, velocity, and displacement capacities of MATS

There are 13 single-end hydro-static or pressure-balanced type of servo-hydraulic actuators in the vertical and lateral axes of the platen. The platen is attached to seven vertical actuators from the bottom, two lateral actuators at each lateral side and two hold-down actuators on the top. The vertical and lateral hydro-static or pressure-balanced type of actuators are anchored to the load frame, but not to the platen. Platen can be sliding on the bearing surface of these actuators during the motion. All these hydro-static and pressure-balanced actuators are almost frictionless when the platen is moving in the longitudinal direction. Fig. 11 shows the allocation of the 13 actuators in the vertical and transverse directions of the MATS. Table 2 shows the specifications for these 13 actuators. On the other hand, longitudinal actuators are mounted between the reaction wall and the platen. The longitudinal actuators can be re-configured by using single or multiple servo-hydraulic actuators, providing the flexibility of MATS to meet various test requirements. Fig. 12 illustrates the six degree of freedoms (DOFs) adopted for MATS. The vertical, pitch and roll DOFs of the platen can be controlled by the seven vertical actuators in the bottom. The lateral and yaw DOFs can be operated by the lateral 4 actuators. With these actuators, the specimen in the MATS can be subjected to a combination of bi-directional shear forces, bi-directional bending moments and vertical load. The full capacities of MATS in each DOF are shown in Table 3. The force and displacement specification in each DOF in detail are given below

Longitudinal direction

Currently, there are two available configurations in the longitudinal direction. In Configuration 1, two or three static actuators are arranged in parallel. The stroke can be either ±1,200 mm or ±700 mm. The peak velocity is 40 mm/sec. The maximum forces can be either 5.08 MN or 7.62 MN in pushing and 3.54 MN or 5.31 MN in pulling. In Configuration 2, two static actuators are replaced with two dynamic actuators. Thus, the maximum stroke and velocity capacity become ±500 mm and 200 mm/sec, respectively. The force capacity is ±2 MN.

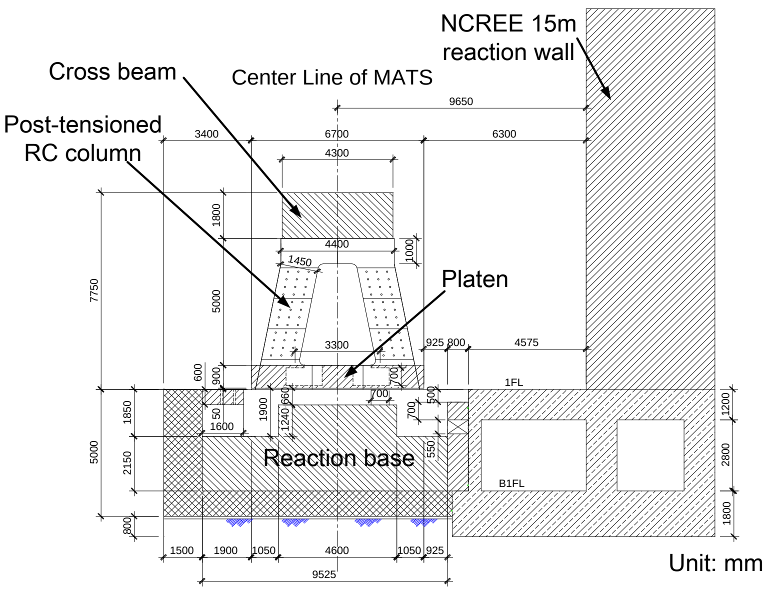

Fig. 10 Schematic of MATS dimensions

Lateral direction

There are four static actuators symmetrically placed at two lateral sides of the platen as shown in Fig. 11. The four lateral actuators are single-end pancake type with pressure-balanced bearing at the interface to the platen. The stroke capacity is ±100 mm. The maximum pushing force of each actuator is 1.9 MN; therefore, the overall lateral force capacity of MATS is slightly less than ±3.8 MN. The maximum velocity can reach up to 20 mm/sec.

Vertical direction

The vertical actuators shown in Fig. 11 can be divided into the bottom and top parts. The bottom actuators include one central static and six side dynamic actuators. The static actuator is a single-end pancake type actuator with the pressure-balanced type bearing at the interface to the platen. The capacity of this static actuator is 30 MN. The six dynamic actuators are the single-end pancake type actuators with hydrostatic bearings at the interface to the platen. Actuator displacement is measured by a Temposonics displacement transducer and force is measured by a pressure transducer. The full capacity of each dynamic actuator is 5 MN. Therefore, the total vertical pushup force capacity can reach 60 MN. The central 30 MN static actuator is turned on when the vertical force requirement is greater than 30 MN. The six side dynamic actuators can be operated independently without turning on the central static actuator. In this manner, without the use of the central static actuator, the maximum velocity can be increased from 5 mm/sec to 30 mm/sec. It should be noted that when any one of these actuators is used, it must be always in contact with the bottom of the platen. For this reason, additional two top hold-down actuators were built-in to allow a peak of 4-MN compressive force to be applied on the top surface of the platen which ensures the bottom actuators can meet the minimum compression force requirements for safety concern. The two hold-down actuators are also single-end pancake type with pressure-balanced bearings at the interface to the platen.

Table 2 Specifications for the vertical, hold down, and lateral actuators

Actuator	Qty	Type	Diameter (mm)	Max. force (kN)	Max. stroke (mm)
Vertical actuator	1	Pressure balanced	1270	30000	125
Vertical actuator	6	Hydrostatic	660.4	5000	125
Hold down actuator	2	Pressure balanced	450.9	2000	125
Lateral actuator	4	Pressure balanced	406.4	1900	±100

Table 3 MATS capacity

DOF	Type	Stroke (mm)	Velocity (mm/s)	Force (MN)
Longitudinal	Static	±1,200 ±700	±40	+5.08 ; -3.54 +7.62 ; -5.31
	Dynamic	±500	±200	±2
Lateral	Static	±100	±20	±3.8
Vertical	Dynamic	+125	±30	+30
	Static	+125	±5	+60
DOF	Type	Stroke (degree)	Velocity (rad/s)	Force (MN-m)
Roll	Dynamic	±2	±0.03	±7.5
Pitch	Dynamic	±2	±0.03	±27
Yaw	Static	±2	±0.015	±5.28

Roll, pitch and yaw directions

For these three DOFs, the maximum rotational capacity is ±2° based on the front end rotational capacity of the vertical and lateral actuators. The velocity capability in the roll and pitch DOFs can reach up to 0.03 rad/sec. Force control mode is not directly provided by the manufacturer; however, it can be performed by using a Simulink model through the SCRAMNet interface. The implementation example is introduced in the coupled steel plate shear wall (C-SPSW) cyclic test later in this paper.

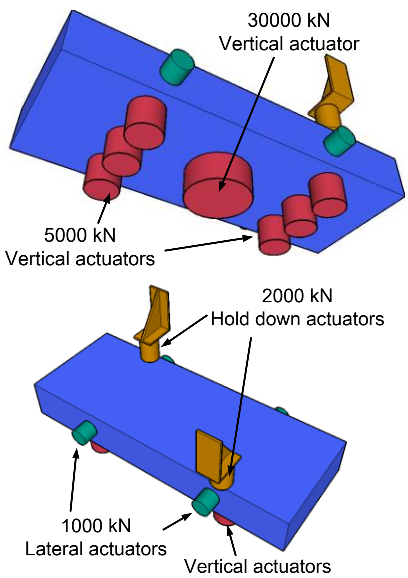

(a) Three-dimensional illustration of the actuators

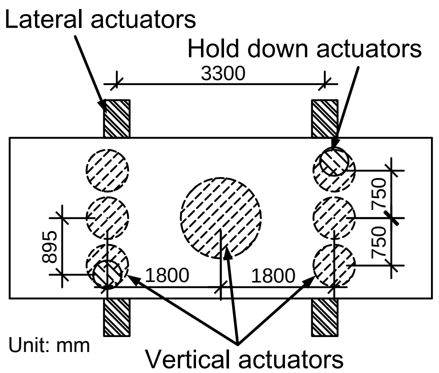

(b) Allocation of the actuators

Fig. 11 Hydro-static and pressure-balanced actuators in MATS

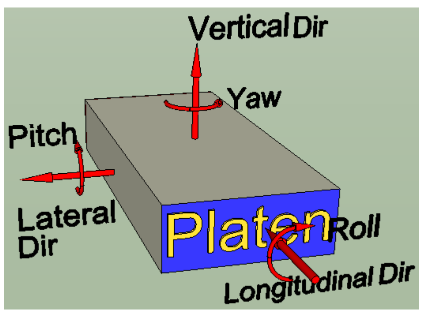

Fig. 12 Definition of degree of freedoms of MATS

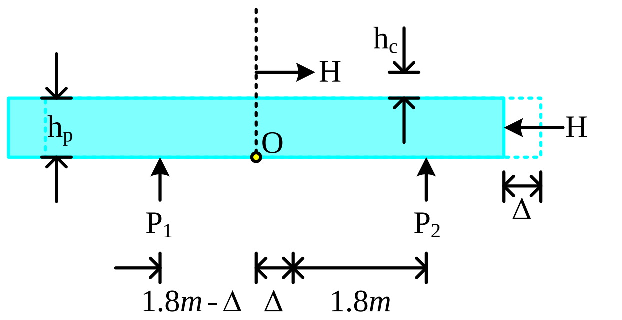

Fig. 13 Free body diagram of a uni-axially loaded member

3.2 Limitation of small axial load

MATS was primarily designed for conducting tests with large compressive force requirements; however, low or zero compressive force may be essential for a few specific tests. For example, damping wall is designed to undergo merely lateral force and rubber bearing installed in the corner of a building may be subjected to very low compression or even tension caused by the overturning moment during an earthquake. Fig. 13 shows the free body diagram of a uni-axially loaded member which was used for determining the actuator performance. The total vertical force is zero. In order to maintain the platen rotation, MATS controller needs to change P_1 and P_2 accordingly. After balancing the moment at the point O resulted from all forces, i.e., $\Sigma M_o=0$, the following equation can be obtained

$$P_1 - P_2 = \frac{-M_H}{1.8} = \frac{-H\left(\frac{h_p}{2}+h_c\right)}{1.8} \tag{2}$$

The notations of P, H, h_c and Δ are identical to those noted in the previous section. It is noted that the total force of hold down actuators is 4000 kN. Meanwhile, the minimum allowable force of each vertical actuator is 133 kN. As a result, the maximum value of P_1 - P_2 is close to 3200 kN when the axial load is approaching to zero. For the tests that require larger moment capacity, additional vertical actuators can be installed on top of the platen to function like hold down actuators. The implementation example is also introduced in the C-SPSW cyclic test later in this paper in which two additional actuators were used to provide a total of 2000 kN hold-down force.

4. Experimental applications

This section introduces various experiments that have been conducted using MATS from simple to complex test setups. First, uni-axial loading tests for buckling restrained brace, concentrically brace, RC column, and bridge deck testing are presented. Second, bi-axially loading tests such as LRB, viscous damping wall, steel panel damper, and RC column testing are described. Furthermore, the application of Shared Common Random Access Memory Network (SCRAMNet) interface with a Simulink-based model for cyclic loading testing of a C-SPSW is illustrated. Last but not least, future potential advanced applications using

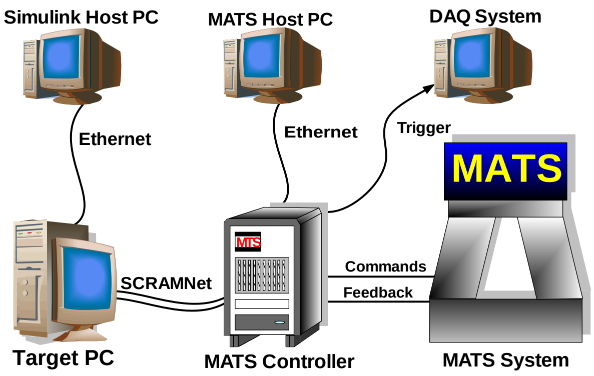

Fig. 14 Hardware and software layout of MATS

MATS are proposed. Fig. 14 shows the framework of the MATS control system. All DOFs are directly controlled by using the Jacobean-matrix transformation which can be calculated from the feedback of actuators. Simple structural testing can be conducted using the prototype control panels; however, numerous control functions are absent and considered essential for complex structural specimens. Consequently, MATLAB/Simulink, xPC Target, Real-time Workshop, and SCRAMNet are available to provide a programmable interface to implement self-developed control algorithms.

4.1 Uni-axial loading tests

Typically, the uni-axial loading tests can be performed in vertical or longitudinal directions. In particular, the loading tests in vertical direction can be treated as pure compressive testing that can be completed straightforwardly and rapidly. The specimens are placed between the platen and the crossbeam with or without shim blocks depending on the specimen height. On the other hand, the specimen is placed between the two longitudinal actuators for the uni-axial loading tests in longitudinal direction. The overturning moment of the platen can be neglected for such testing. In addition, for the specimen longer than 7 meters, it can be placed on the platen at one end and connected to the reaction wall at the other end. However, the induced overturning moment at the platen needs to be controlled. Representative uni-axial loading tests are introduced in the following.

RC column and bridge deck

RC column compressive testing is considered as the most typical type for uni-axial loading testing in vertical direction. Full-scale RC column specimens with high performance concrete and high strength reinforcements are frequently conducted using MATS because the maximum vertical force of MATS can be up to 60 MN. In addition, the clear space of MATS can be up to 5 meters which is more than enough to install a full-scale RC column. Fig. 15 shows two typical RC column compressive tests in which the left-hand side is a simple RC column while the right-hand side is a RC column retrofitted by thin steel plates. Fig. 16 shows a bridge deck test in which a pre-stressed girder with corrugated steel web was designed for the bridge. The maximum loading capacity of the novel design of bridge can be obtained by conducting compressive testing, demonstrating that MATS is appropriate for testing to evaluate the performance of bridges with high strength and large dimension.

Buckling restrained brace and concentrically brace

MATS can be configured for conducting horizontal-axially loading tests for braces and viscous dampers as shown in Fig. 17 in which a double tube buckling restrained brace (BRB) is placed between the two longitudinal actuators. Fig. 18 shows the test setup of a concentrically brace which was a component test of a full-scale three-story concentrically braced frame test conducted in NCREE (Tsai *et al.* 2012).

Fig. 15 Test setup for RC column compressive tests

Fig. 16 Test setup of a bridge deck test

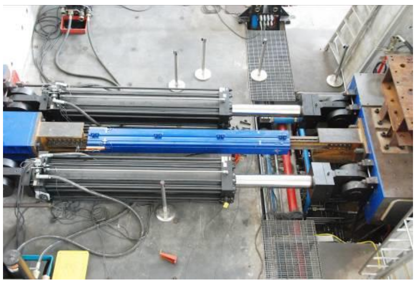

Fig. 17 Test setup of a BRB test

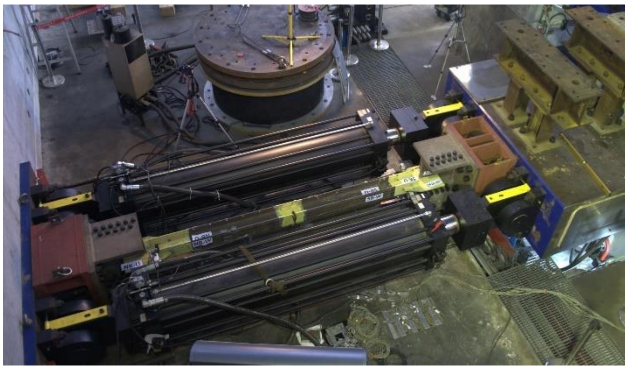

Fig. 18 Test setup for a concentrically brace

4.2 Bi-axially loading tests

The bi-axially loading tests are usually conducted with vertical actuators in force control and longitudinal or lateral actuators in displacement control. In some cases, longitudinal and lateral actuators are displacement-controlled simultaneously to simulate the seismic behavior of the components during earthquakes such as steel panel dampers. Representative bi-axially loading tests are described afterwards.

Lead rubber bearing

Lead rubber bearings (LRB) have been widely applied to buildings and bridges to isolate the earthquake excitation; therefore, the corresponding experimental demands have been increasing year by year. However, most of the performance tests were conducted in reduced-scale due to the limitation of test facilities (Kim *et al.* 2014). On the other hand, full-scale LRB testing can be performed on MATS as it was designed for testing full-scale base isolation devices. Fig. 19 shows the typical experimental setup of a LRB using MATS. Generally, the height of a LRB is much shorter than the clear height of MATS; therefore, the installation of RC shim blocks and steel plates are necessary for a LRB test. According to the seismic building code requirements in Taiwan, a LRB needs to be subjected different levels of constant vertical loads with altered magnitudes and frequencies of sinusoidal displacement in horizontal direction. Many prototype LRB tests have been completed using MATS.

Viscous damping wall and steel panel damper

The experimental setups of viscous damping walls and steel panel walls are identical as shown in Fig. 20. The RC shim blocks or the steel reaction beams are required to adjust the position of the test specimens. The specimen is placed vertically and anchored between the RC blocks and the platen which is similar to the setup for LRBs. However, zero vertical loading is sustained during the test for both viscous damping walls and steel panel walls. Viscous dampers are considered one of the rate-dependent devices; therefore, high-speed actuators are indispensable in order to satisfy the velocity requirements. Sinusoidal displacements are imposed on the specimen. On the other hand, steel panel dampers are not rate-dependent devices; therefore, incremental cyclic displacement profiles can be applied to the specimen quasi-statically.

RC column

Experiments of RC columns subjected to high axial forces and single-curvature moments have been conducted to explore the propagation of plastic hinge length. However, in some test cases, it is intended to have RC columns be subjected to axial forces and reverse-curvature moments to simulate the real conditions of RC columns (Wang *et al.* 2015). In particular, high axial force is required for evaluating the performance of high strength RC columns (Bhayusukma and Tsai 2014). Fig. 21 shows the experimental setup on MATS for a RC column subjected to high axial force and horizontal displacement simultaneously. Similar to the test setup for damping walls, RC columns can be anchored between the RC blocks and the platen. However, the vertical force imposed on the RC column is significant as columns take the gravity load of the structure. The vertical force is applied to the column incrementally and remained constant during the test. Incremental cyclic displacements are then applied to the column until damage and failure can be observed.

Fig. 19 Test setup of a LRB performance test

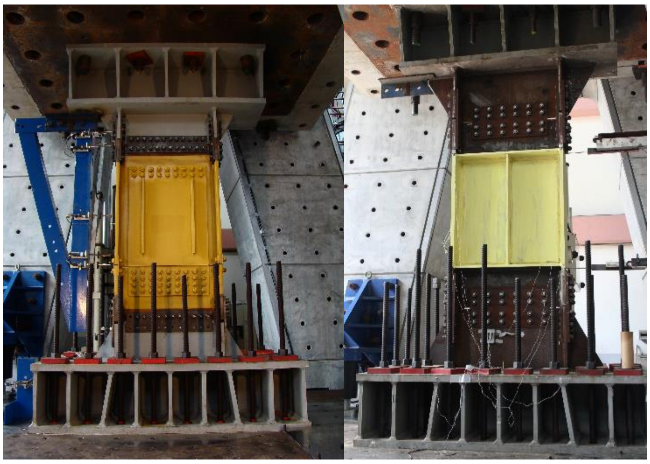

(a) (b)

Fig. 20 Test setup of (a) a viscous damping wall; (b) a steel panel wall

Fig. 21 Test setup for a bi-axial RC column test

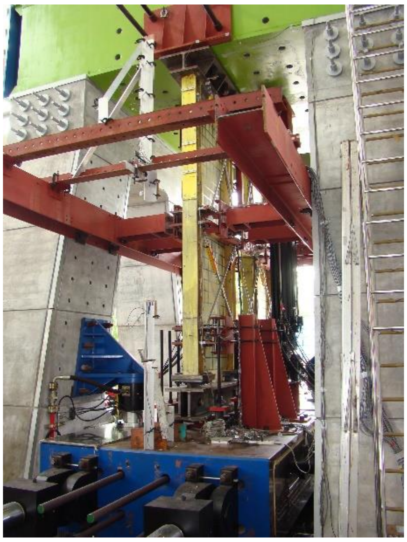

Fig. 22 Test setup of a C-SPSW substructure test

4.3 Coupled steel plate shear wall

A coupled steel plate shear wall (C-SPSW) was designed and tested using MATS which is considered as the most complex experiment that has ever been conducted using MATS for the past decades. It was designed for the transverse direction of a six-story prototype building (Li *et al.* 2012). One of the C-SPSWs was cut at the third story into a substructure and reduced to a 40% scale specimen. The 0.4-scale bottom two and half stories C-SPSW substructure was installed upside down between the cross beam and the platen. The specimen was required to resist the vertical loads, the lateral seismic shear and the overturning moment transmitted from the upper stories of the six-story building. It was hypothesized that the lateral force distribution was an inverted triangular shape and the lateral seismic shear forces at the lowest two floors were ignored. Thus, the overturning moment at the section cut of the specimen was 2.51-meter times of the shear force in the specimen. According to the hydraulic pressure (3000 psi) of MATS, the top two hold-down actuators could only provide 2800-kN compressive force on the platen. However, the applied overturning moment must not result in any of the bottom dynamic actuators to undergo tension when the lateral displacement of the specimen became large. Hence, there were two additional vertical static actuators installed between the cross beam and the platen to provide a total of 2000 kN. These two static actuators supplemented the hold-down actuators in balancing the bottom six dynamic actuators. Fig. 22 illustrates the experimental setup of the C-SPSW testing.

The test was conducted by a pitch force control model programmed in MATLAB/Simulink. It provides an interactive graphical environment and a series of block libraries for design, simulation, and implementation. The test was running in a real-time environment provided by xPC Target which communicated with the MATS controller through SCRAMNet. Meanwhile, the predefined displacement profile was also programmed using MATLAB/Simulink and sent to the MATS controller through SCRAMNet. When the longitudinal actuators reach any displacement in each step, the pitch force feedback (overturning moment) and the longitudinal force feedback were continuously transmitted at a frequency of 1024 Hz to the Target PC through the optical cables. The pitch force command was then computed using the longitudinal force feedback and applied immediately to the specimen. The technical information can be found in the reference (Chen *et al.* 2009).

4.4 Potential advanced applications

Owing to the development of hybrid simulation and online model updating techniques (Mahin and Shing 1985, Shing *et al.* 1996, Elanwar and Elnashai 2014, Hashemi *et al.* 2014), various advanced experiments may be conducted using MATS in the future. The concept of hybrid simulation for structural engineering studies can be traced back to early 1970s. After the developments and exploration from the academic researchers and industrial engineers in the following decades, hybrid simulation has been recognized as one of the powerful testing methods to investigate the seismic responses of structures subjected to earthquake ground motions. In this approach, a structure is divided into two or more parts: one part of the structure is tested physically and the remainder is modeled numerically. In particular, the physical specimen is the portion of structure which is difficult to model numerically. The equation of motion is solved by employing step-by-step integration methods. Several integration algorithms have been proposed and developed for hybrid simulation with nonlinear structural behavior (Chang 2002, Chang 2007, Chen and Ricles 2008, Ahmadizadeh and Mosqueda 2008, Hung and El-Tawil 2009, Mosqueda and Ahmadizadeh 2011). Furthermore, the criteria for the selection of the time integration schemes have been suggested by conducting numerical simulation (Verma *et al.* 2015). On the other hand, hybrid simulation with online model updating was a novel idea in order to improve the consistency among substructures. This method was focused on the structural systems with repeated components; for instance, an expressway with a large number of duplicated piers. Apparently, it is not practical to construct physical specimens for all of these piers. Model updating method is to test one of these piers and online modify the predefined parameters of the other piers which are numerically simulated based on the experimental data. In this section, potential future application of hybrid simulation with online model updating on MATS is introduced conceptually.

Past experimental researches regarding seismic isolation are restricted to scale-down seismically isolated structural models tested with shaking table systems. Typically, the seismic response of full-scale isolators is a combination of shear deformation, up-lift, and rotation response, which cannot be considered in current available commercial computational tools. However, a full-scale isolator can be tested using MATS as mentioned in the previous section. Therefore, hybrid simulation with online model updating provides an alternative solution to investigate the seismic response of a base-isolated building as illustrated in Fig. 23. The superstructure is simulated by a sophisticated numerical model, which can be highly nonlinear. One of the isolators is physically tested in six degree-of-freedom displacement control using MATS. The other isolators are initially simulated by a preliminary numerical model and updated online during the test. Fig. 24 shows the block diagram of the hybrid simulation with online model updating of a base-isolated building where $\mathbf{x}_d$ and $\mathbf{x}_E$ represent the desired and measured displacements of the physical tested isolator. Meanwhile, $\mathbf{r}_E$, and $\mathbf{r}_M$ are the restoring force of the tested and simulated isolators, respectively. An additional parameter analysis module developed by NCREE can be used to calculate a set of parameters for the numerical model based on the experimental data (Yang *et al.* 2012). Accordingly, $\mathbf{p}_M$ is the identified parameters for the simulated isolators. The feasibility and reliability of the parameter analysis module has been demonstrated in a software-based manner. The real application on MATS including the design and implementation of the software and parameter analysis module may be carried out in the near future.

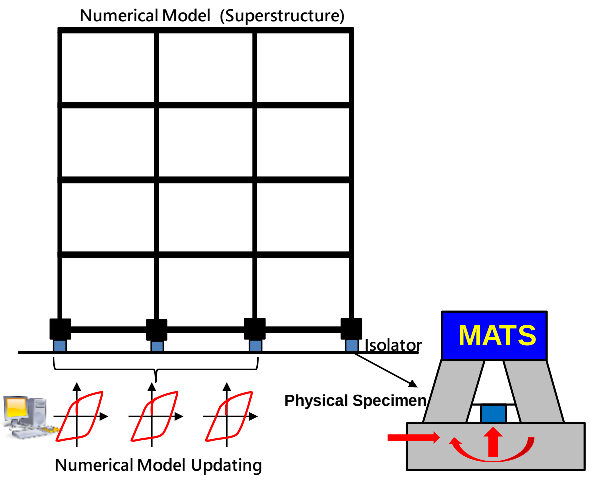

Fig. 23 Schematic of hybrid simulation with online model updating of a base-isolated building

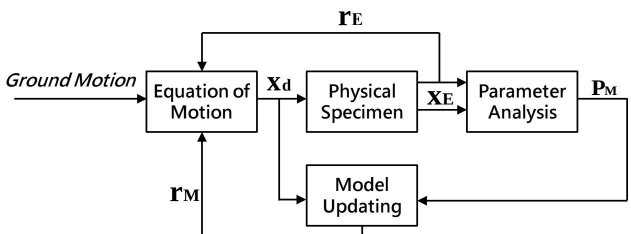

Fig. 24 Block diagram of hybrid simulation with online model updating

5. Conclusions

The multi-axial testing system (MATS) is a unique and complex experimental system for earthquake engineering studies. The establishment of MATS enhances the experimental research capacity of NCREE laboratory and solves qualification issues of engineering practices for seismically resistant or isolated devices. A large variety of experiments with different requirements have been successfully implemented and completed for the past decades including structural members, energy dissipation devices, isolators, and substructures, providing extensive experience in the field of experimental earthquake engineering. In addition, advanced experimental control technique has been effectively applied to MATS to complete a complex substructuring test. It appears that this experimental technique could be extended to a more general experimental control framework, such as hybrid simulation with model updating in the future.

Acknowledgments

The authors would give sincere appreciation to Professor Keh-Chyuan Tsai from the Department of Civil Engineering, National Taiwan University for his supervision of MATS analysis and testing. Meanwhile, the authors would like to thank MTS Systems Corporation and Ruentex Corporation for designing the hydraulic control system and the details of the MATS frame, respectively.

References

Ahmadizadeh, M. and Mosqueda, G. (2008), "Hybrid simulation with improved operator-splitting integration using experimental tangent stiffness matrix estimation", *J. Struct. Eng.*, ASCE, **134**(12), 1829-1838.

Bhayusukma, M.Y. and Tsai, K.C. (2014), "High-strength RC columns subjected to high-axial and increasing cyclic lateral loads", *Earthq. Struct.*, **7**(5), 779-796.

Chang, S.Y. (2002), "Explicit pseudodynamic algorithm with unconditional stability", *J. Eng. Mech.*, **128**(9), 935-947.

Chang, S.Y. (2007), "Enhanced, unconditionally stable, explicit pseudodynamic algorithm", *J. Eng. Mech.*, **133**(5), 541-554.

Chen, C. and Ricles, J.M. (2008), "Development of direct integration algorithms for structural dynamics using discrete control theory", *J. Eng. Mech.*, **134**(8), 676-683.

Chen, P.C., Tsai, K.C., Chen, J.C. and Lin, T.H. (2009), "Advanced seismic experiments using SCRAMNet: an example on the cyclic test of a coupled-SPSW substructure", *Proceedings of the 22th KKCNN Symposium on Civil Engineering*, Chiangmai, Thailand, November.

Elanwar, H.H. and Elnashai, A.S. (2014), "On-line model updating in hybrid simulation tests", *J. Earthq. Eng.*, **18**(3), 350-363.

Hashemi, M.J., Masroor, A. and Mosqueda, G. (2014), "Implementation of online model updating in hybrid simulation", *Earthq. Eng. Struct. D.*, **43**(3), 395-412.

Hung, C.C. and El-Tawil, S. (2009), "Full operator algorithm for hybrid simulation", *Earthq. Eng. Struct. D.*, **38**(13), 1545-1561.

Kim, D., Oh, J., Do, J. and Park, J. (2014), "Effects of thermal aging on mechanical properties of laminated lead and natural rubber bearing", *Earthq. Struct.*, **6**(2),127-140.

Li, C.H., Tsai, K.C., Chang, J.T., Lin, C.H., Chen, J.C., Lin, T.H. and Chen, P.C. (2012), "Cyclic test of a coupled steel plate shear wall substructure", *Earthq. Eng. Struct. D.*, **41**(9), 1277-1299.

Mahin, S.A. and Shing, P.B. (1985), "Pseudodynamic method for seismic testing", *J. Struct. Eng.*, **111**(7), 1482-1503.

Mosqueda, G. and Ahmadizadeh, M. (2011), "Iterative implicit integration procedure for hybrid simulation of large nonlinear structures", *Earthq. Eng. Struct. D.*, **40**(9), 945-960.

Rich, R.T. (1998), "Platen design for the seismic response modification device testing facility", Report No. SSRP 98/07, University of California, San Diego.

Shing, P.B., Nakashima, M. and Bursi, O.S. (1996), "Application of pseudodynamic test method to structural research", *Earthq. Spectra*, **12**(1), 112-141.

Tsai, C.Y., Tsai, K.C., Ao, W.H., Roeder, C.W., Mahin, S.A., Lin, C.H., Yu, Y.J., Wang, K.J., Wu, A.C., Chen, J.C. and Lin, T.H. (2012), "Seismic design and hybrid tests of a full-scale 3-story concentrically braced frame using in-plane buckling braces", *Earthq. Spectra*, **29**(3),1043-1067.

Verma, M., Rajasankar, J. and Iyer, N.R. (2015), "Numerical assessment of step-by-step integration methods in the paradigm of real-time hybrid testing", *Earthq. Struct.*, **8**(6), 1325-1348.

Wang, P., Shi, Q.X., Wang, Q.W. and Tao, Y. (2015), "Experimental behavior and shear bearing capacity calculation of RC columns with a vertical splitting failure", *Earthq. Struct.*, **9**(6), 1233-1250.

Yang, Y.S., Tsai, K.C., Elnashai, A.S. and Hsieh, T.J. (2012), "An online optimization method for bridge dynamic hybrid simulations", *Simulat. Model. Practice Theory*, **28**, 42-54.

KT